Fabrication of Photonic Crystal Slabs and Defects using Laser Interference Lithography and Focused Ion Beam-Assisted Deposition

René M. de Ridder, Cazimir G. Bostan, Henk A.G.M. van Wolferen, Inge van Dorssen, Laura Vogelaar*, Frans B. Segerink*, Laurens Kuipers*, and Niek F. van Hulst*

Lightwave Devices Group
**Applied Optics Group*
University of Twente, MESA+ Research Institute,
P.O. Box 217, 7500 AE Enschede, the Netherlands
Tel: +31 53 489 2712, Fax: +31 53 489 3343, E-mail: R.M.deRidder@utwente.nl

ABSTRACT
A method is described for fabricating photonic crystal slabs, using a combination of laser interference lithography for generating a regular periodic structure (the crystal lattice), and focused ion beam-assisted deposition for defining defects in this lattice, which may act as waveguides or resonators. As an example, results will be shown of a photonic crystal slab with a line defect in silicon nitride.
Keywords: Photonic Crystals, Photonic Bandgap structures (PBG), Optical waveguide components, Interference lithography, Holographic lithography, Ion beam-assisted deposition.

1. INTRODUCTION

Photonic crystals are structures having a periodic variation of the refractive index with a period in the order of the wavelength of the electromagnetic waves for which they are designed, see e.g. [1]. These structures can be designed to have a photonic bandgap, i.e. a band of frequencies that cannot propagate through it. Photonic crystal slabs consist of a layer of high refractive index material which is perforated with a regular array of holes filled with air or another low-index material, see e.g. [2]. Wave propagation in the bandgap of a photonic crystal may be possible along a defect, for example a narrow region where the crystal structure has been removed, e.g. [3]. A line defect in a photonic crystal slab may guide a wave by confining it in lateral directions (in-plane) by its photonic bandgap, and in the out-of-plane direction by the mechanism of total internal reflection, thus forming a waveguiding channel which can have extremely sharp bends (bending radius of the order of a wavelength), allowing very compact folding of waveguides, e.g. [4]. Also, high-quality optical microresonators can be realised as defects in a photonic crystal, which may lead to very compact optical wavelength filters and add-drop multiplexers for optical communications [5,6].
Probably the most widely used method for defining (quasi) two-dimensional photonic crystal structures is direct writing e-beam lithography. Although this method is very flexible, allowing the definition of arbitrary patterns, it is not very efficient for defining extended periodic structures like photonic crystals, due to its sequential writing character. A suitable method for fabricating these extended structures at once is laser interference lithography (LIL), also known as holographic lithography [7,8,9]. A limitation of this method is that only regular patterns can be fabricated, so that more interesting structures with defects that can act as waveguides and resonators are hard to obtain. Due to the required alignment accuracy of the defects with respect to the photonic crystal, conventional lithography cannot be used. However, using an accurately focused ion beam (FIB) [10], thin metal layers can be deposited very locally [11]. Since by scanning the ion beam a secondary electron emission image of the photonic crystal can be formed, it is possible to align the FIB deposition accurately with respect to the crystal. Like e-beam lithography, FIB-deposition is a sequential write process, but for defining defects this is much less of a drawback since defects typically take up only a small fraction of the crystal surface. By first creating a metal mask with a regular lattice of holes, using LIL and lift-off, then selectively filling holes using FIB-assisted platinum deposition, and finally using the resulting metal pattern as an etch mask for the dielectric slab, a photonic crystal slab with well-aligned defects can be fabricated [12]. The procedure will be explained in detail below, and some results will be shown.

2. LASER INTERFERENCE LITHOGRAPY

The most straightforward implementation of LIL consists in a 2-beam interferometer in which two coherent wave fronts are combined to form a sinusoidal interference pattern in space. By exposing a layer of resist to this pattern, a simple one-dimensional grating can be generated. We used a simple and stable Lloyd's mirror set-up where an approximately plane wave reaches a photosensitive layer (photoresist) on a substrate both directly and

0-7803-7375-8/02/$17.00

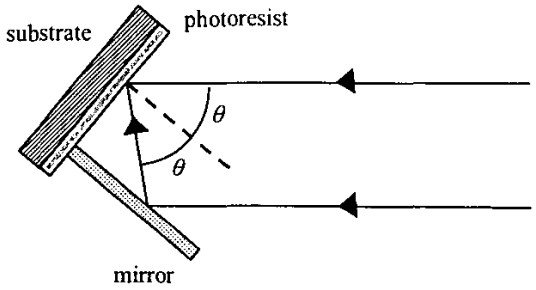

Figure 1. Lloyd's mirror interferometer set-up.

via a mirror which is oriented perpendicular to the substrate (Fig. 1). The angle of incidence θ, and thus the periodicity of the interference pattern, is easily adjusted by rotating the substrate+mirror assembly as a whole with respect to the exposure beam. The light source is an argon laser at 364.8 nm UV wavelength (I-line), of which the beam is spatially filtered through a 10 μm pinhole at a relatively large distance of 2.0 m from the substrate, leading to a beam non-uniformity better than 10% and deviations in the angle of incidence less than 2° over the 70 mm useful diameter of the substrate+mirror assembly.

By overlaying multiple exposures or by combining more than two beams, more complex two-dimensional (2D) structures can be patterned including square arrays of dots or holes.

In this paper we consider a LIL process involving the overlap of two exposures oriented at 60 degrees with respect to each other (see Fig. 2). Our aim is to use the photoresist pattern as a template for fabricating a 2D photonic crystal slab with a triangular lattice of cylindrical holes in silicon and silicon nitride slabs.

For the second exposure the angle of incidence θ remains the same but the substrate is rotated over an angle $\alpha = 60°$. Both linear gratings have the same period d,

$$d = \frac{\lambda_0}{2\sin\theta} \tag{1}$$

where λ_0 is the free-space wavelength of the exposure radiation. It can be seen that the smallest theoretical period ($\lambda_0/2$) is achieved for grazing incidence; however, this is not realistic, since in that case the incident irradiance will be zero. The lattice constant a of the triangular lattice will be

$$a = \frac{d}{\sin 60°} \tag{2}$$

From the point of view of quasi-2D photonic crystal applications, there are two important aspects: (1) the periodicity of the lattice should be perfect, and (2) the 'filling factor' should be uniform over a large area.

The first requirement is easily satisfied, being an intrinsic property of LIL. The second one is a challenge, because it is related to the geometry of the photoresist template obtained after the development process. It requires fine-tuning of the photolithographic parameters (e.g. irradiance, exposure time).

In order to get a starting point in the design of LIL process we performed calculations of the electromagnetic dose recorded in the photoresist layer, taking into account the geometrical and optical properties of the materials involved.

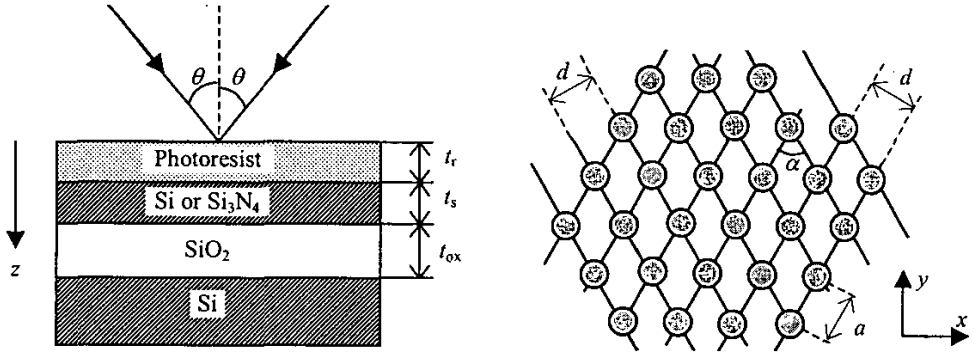

Figure 2. Lithography scheme. Left: cross-section of a silicon wafer with a high-refractive index slab on a buffer layer, with photoresist on top. Right: top view of the 2D periodic structure resulting from superimposing two LIL exposures.

Photoresist is an absorbing material with a refractive index $n_f \cong 1.7$ and the extinction coefficient $k_f \cong 0.02$. Common photoresist materials show 'bleaching', i.e. saturation of absorption as electromagnetic radiation is absorbed (k_f decreases during the exposure process, typically by one order of magnitude).
The interference pattern in the photoresist layer is more complicated than suggested by equation (1). There is also a standing wave pattern perpendicular to the substrate plane, caused by multiple reflections at the interfaces between layers. The photoresist layer can be regarded as an asymmetric Fabry-Perot etalon, bounded by air at one side and by the multilayer stack at the other.

The recorded dose in the photoresist can be calculated from the **irradiance distribution** $I(x,y,z)$, given as:

$$I(x,y,z) = I_0 \cos\theta f_1(x,y) f_2(z) \qquad [\mathrm{W\,m^{-2}}] \tag{3}$$

where I_0 is the irradiance of the exposure beam in air for normal incidence, θ the angle of incidence, f_1 and f_2 are dimensionless periodic distribution functions, with $f_1(x,y)$ the periodic effective in-plane distribution due to the cumulative effect (sum) of the two exposures, and $f_2(z)$ the vertical distribution due to interfering reflections. Taking into account that $k_f << n_f$, we can approximate the spatial period Λ_z of $f_2(z)$ as:

$$\Lambda_z = \frac{\lambda_0}{2 n_f \cos\theta_f} \tag{4}$$

where θ_f is the refraction angle at the air-photoresist interface.
The **absorbed energy density** in photoresist can be calculated by considering the conservation of energy using Poynting's theorem, leading to:

$$Q(x,y,z) = 2k_0 n_f k_f I(x,y,z) \qquad [\mathrm{W\,m^{-3}}] \tag{5}$$

where $k_0 = 2\pi/\lambda_0$.
Finally, the **recorded dose density** is obtained by integrating the absorbed energy Q in time:

$$D(x,y,z) = 2k_0 n_f I(x,y,z) \int_0^{t_{ex}} k_f(t)\,dt \qquad [\mathrm{J\,m^{-3}}] \tag{6}$$

where t_{ex} is the exposure time. A typical calculated distribution is shown in Fig. 3.

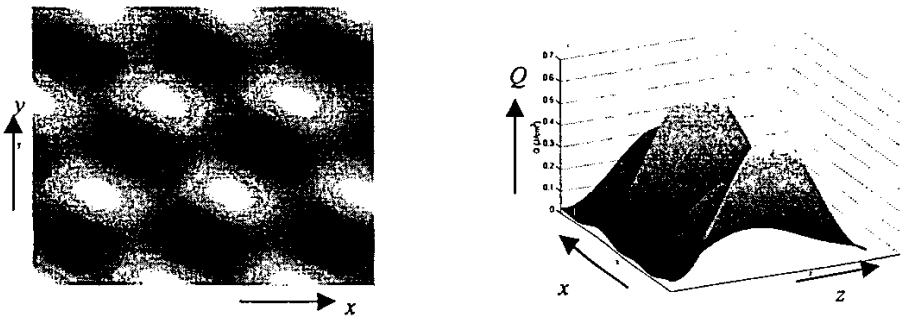

Figure 3. Calculated absorbed dose density. Left: top view at resist-air interface. Right: standing wave pattern (side-view; structure is 122 nm (t_r =0.3 λ_0) photoresist on SOI wafer with silicon slab thickness t_s = 300 nm, and oxide thickness t_{ox} = 700 nm).

2.1 Antireflection coatings

The strong UV reflection at the silicon-resist interface, leads to a vertical standing wave pattern $f_2(z)$ in the resist, as shown in Fig. 3, right. After development, pillars will remain having a vertical modulation of their diameter, see Fig. 4, left. In case of a positive photoresist an undercut resist profile results if the maximum of the standing wave occurs at the resist/substrate interface. Such a profile would be suitable for lift-off, but unfortunately is usually mechanically unstable. In order to be able to later invert the resist pattern (holes in stead of pillars) using lift-off, the resist should be completely removed from the Si-interface. This leads to a tendency of over-exposure or over-development of the resist, resulting in weak low-diameter sections in the pillars, where they may easily break. Also, if there is a significant thickness nonuniformity of the resist layer, a vertical standing wave pattern can result in large variations in the developed line widths.

To minimize the effect of the standing wave pattern there are two solutions: (1) use an antireflection coating (ARC) between the photoresist and silicon layers, and (2) use a resist thickness of less than half the wavelength of the standing wave pattern (Λ_z = 100 nm, in our case), in order to obtain more robust pillars. ARC layers can be either absorptive (based on organic materials) or interferential (based on dielectrics). The interference type

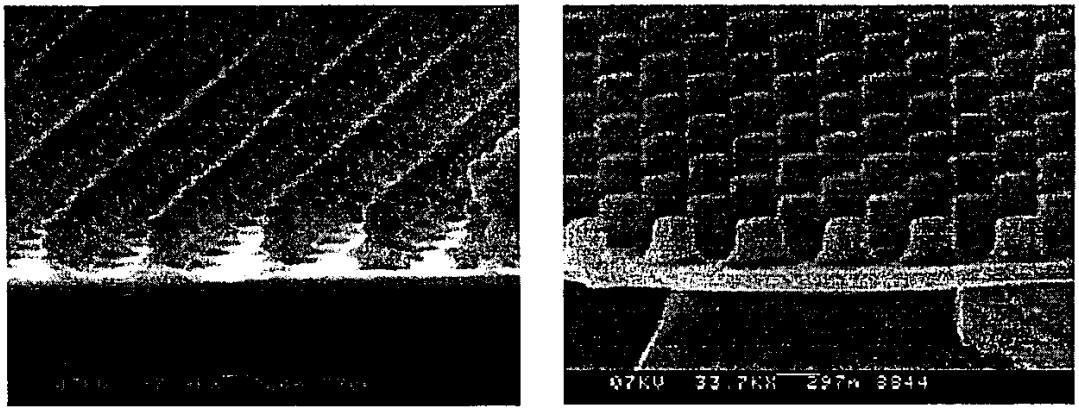

Figure 4. SEM images of photoresist (300 nm Olin907/12, developed with OPD-4262 for 10 s) patterns on silicon, obtained by LIL (beam intensity I_0 = 89 $\mu W\ cm^{-2}$). Left: square lattice, a=600 nm (θ = 17°), 80 s exposure time, without ARC. Right: triangular lattice, a=560 nm (θ = 22.1°), 110 s exposure time, with ARC.

filter approach is an attempt to *optimise* the interference phenomenon, while the bottom antireflection coating (BARC) relies on absorption to reduce substrate reflection and therefore *eliminates* interference effects. Using an organic ARC may cause problems since it needs to be removed before depositing a metal layer for lift-off in the next processing step. An additional dielectric layer is also a technological complication.

2.2 Three-beam interference

As can be seen from Fig. 3, the shape of the recorded dose distribution due to the double exposure method will be elliptical. In principle, circular shapes can be produced by adding a third exposure after turning the substrate another 60°, but in practice this cannot be accomplished since the third exposure should be well-aligned with respect to the pattern resulting from the first two exposures. A better approach is to generate an interference pattern of three coherent beams. A very elegant way of generating these beams has been described by Berger et al. [8]. It involves using a collimated laser beam incident on a mask containing three diffraction gratings positioned on the sides of an equilateral triangle. The first order diffracted waves interfere in the wafer's plane (which is parallel to the plane of the mask) producing a triangular lattice.

The three-wave interference approach has several interesting features: (1) single-step exposure, (2) circular shape of the resist pattern, (3) increased spatial dose contrast which may allow direct creation of a hole pattern in positive resist without the need of lift-off, (4) lattice constant depending only on the mask grating pitch (not on wavelength or mask-substrate distance). The latter feature is a mixed blessing: it provides for a very stable process, but it also reduces experimental flexibility (for each lattice constant a different grating structure should be fabricated). For this reason, the method has not been used in the work described here.

3. FOCUSED ION BEAM-ASSISTED DEPOSITION

After fabricating a resist dot pattern as shown in Fig. 4, a very thin chromium layer (20 nm) is evaporated on top of the resist pattern. This layer does not cover the 'vertical' resist walls, so if the sample is immersed in acetone, the resist will dissolve, in the course lifting off the metal on top, so that only the metal between the resist dots remains. This metal now forms a pattern of holes, so that it can be used as an etch mask for generating a hole pattern in the slab below, thus creating a photonic crystal slab. In order to create defects in this photonic crystal slab, the etch mask should be locally modified.

A focused ion beam (FIB) system can be used for both local etching and metal deposition, which has made it a valuable tool for repairing photolithographic masks and electronic circuit chips. We used an FEI 200 FIB system. With its steerable beam of Ga^+ ions that can be focused to a diameter of about 7 nm, such a system could in principle be used for directly etching the hole pattern into the slab. However, since covering a large area with holes would require mechanical translation of the substrate, so-called stitching errors will occur which form unwanted photonic crystal defects. Also, etching millions of holes would take a very long processing time. Therefore, we have used the technique for modifying a metal etch mask after the regular hole pattern has been formed by LIL and lift-off. A platinum-containing organic gas $(CH_3)_3(CH_3C_5H_4)Pt$ decomposes due to the action of the ion beam so that Pt is locally deposited where the beam scans the structure. In this way, holes in the Cr mask can be selectively filled with a thin (50 nm) Pt layer. The location of the deposition can be very accurately

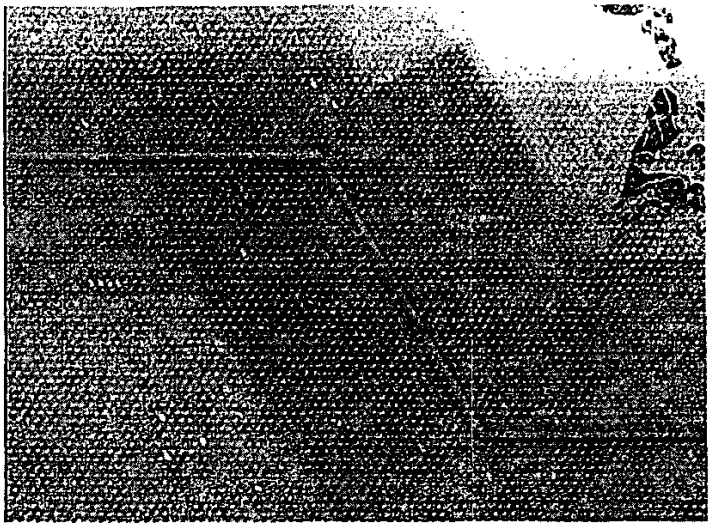

Figure 5. Scanning FIB image of triangular hole pattern (a=560 nm) in Cr mask, with line defect made by FIB-assisted Pt deposition filling selected holes.

aligned, since the scanning ion beam generates electron emission from the substrate, which can be used for image formation just as in an SEM.

Figure 5 shows the resulting metal mask including line defects, as imaged using this scanning FIB mechanism. The image shows also a drawback of the imaging method: the scanning FIB etches while imaging; the large dark squares result from previous imaging at a higher magnification, which was necessary for aligning the defects with respect to the hole pattern.

4. ETCHING THE PHOTONIC CRYSTAL STRUCTURE

For a photonic crystal structure, a large refractive index contrast is needed for obtaining an appreciable band gap. We fabricated two different kinds of structures: (1) a 146 nm thick free-standing Si_3N_4 ($n = 2.16$ @ $\lambda = 670$ nm) photonic crystal slab in air with triangular lattice parameter $a = 300$ nm for operation in the visible spectrum, and (2) a triangular lattice of holes ($a = 560$ nm) in crystalline Si ($n \cong 3.5$ @ $\lambda = 1550$ nm), as a first step in fabricating a photonic crystal slab in an SOI wafer for operation at telecom wavelengths around 1550 nm. In both cases, the pattern in the metal layer is transferred to the high-index layer below by reactive-ion etching (RIE) using a CHF_3/O_2 plasma. In the case of the Si_3N_4 slab, this is followed by a wet chemical etch in buffered HF, which under-etches the nitride layer through the holes, removing the SiO_2 buffer layer below so that a free standing structure remains. Some results are shown in Figures 6 and 7. The first optical measurements on the nitride slab structure will be presented in a different contribution to this Symposium [13].

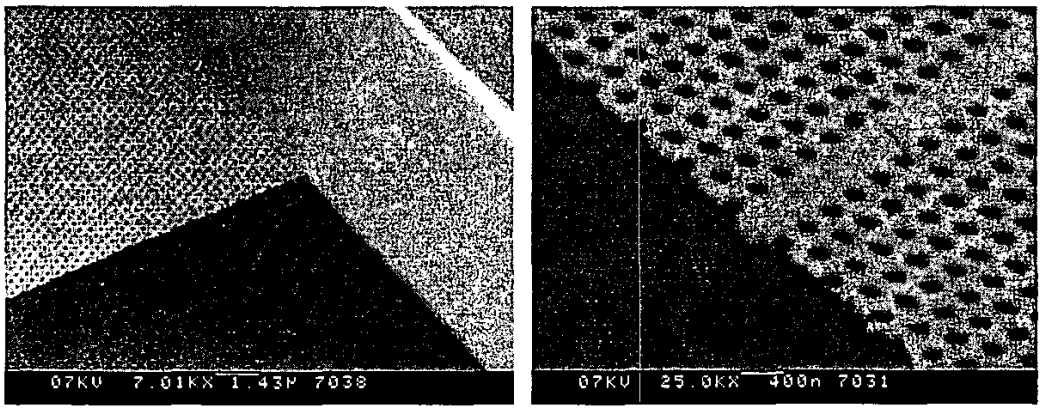

Figure 6. SEM images of silicon nitride photonic crystal slab. Left: free-standing slab. Right: detail showing line defect.

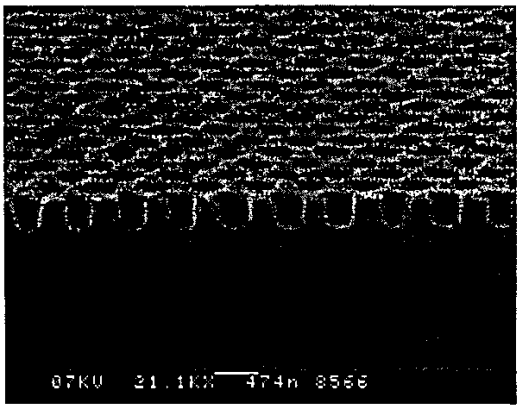

Figure 7. SEM image of hole pattern in silicon.

5. CONCLUSIONS

A model has been presented for calculating the recorded dose density function in laser interference lithography. We have shown that the LIL method is very suitable for fabricating regular arrays of holes in thin slabs of high refractive index material, thus forming photonic crystal slabs. This method was successfully combined with FIB-assisted Pt deposition on metallic etch masks, which enables the introduction of local defects in the crystal.

ACKNOWLEDGEMENT

The authors would like to thank Lucie Hilderink for depositing the optical thin films, and Bert Otter and Mark Smithers for providing the SEM images.

REFERENCES

[1] J.D. Joannopoulos, R.D. Meade, J.N. Winn, *Photonic crystals: Molding the flow of light*, Princeton, NJ: Princeton University Press, 1995.

[2] H. Benisty, C. Weisbuch, D. Labilloy, M. Rattier, C.J.M. Smith, T.F. Krauss, R.M. De la Rue, R. Houdre, U. Oesterle, C. Jouanin, D. Cassagne: Optical and confinement properties of two-dimensional photonic crystals, *J. Lightwave Technol., vol. 17, pp. 2063-2077, 1999.*

[3] S.G. Johnson, P.R. Villeneuve, S.H. Fan, J.D. Joannopoulos: Linear waveguides in photonic-crystal slabs, *Phys. Rev. B, vol. 62, pp. 8212-8222, 2000.*

[4] A. Chutinan, S. Noda: Waveguides and waveguide bends in two-dimensional photonic crystal slabs, *Phys. Rev. B, vol. 62, pp. 4488-4492, 2000.*

[5] S. Fan, P.R. Villeneuve, J.D. Joannopoulos, H.A. Haus: Channel drop tunneling through localized states, *Phys. Rev. Lett., vol. 80, pp. 960-963, 1998.*

[6] R. Stoffer, H.J.W.M. Hoekstra, R.M. de Ridder, E. van Groesen, F.P.H. van Beckum: Numerical studies of 2D photonic crystals: Waveguides, coupling between waveguides and filters, *Optical and Quantum Electronics, vol. 32, pp. 947-961, 2000.*

[7] S.C. Kitson, W.L. Barnes, J.R. Sambles: The fabrication of submicron hexagonal arrays using multiple-exposure optical interferometry, *IEEE Photonics Technol. Lett., vol. 8, pp. 1662-1664, Dec. 1996.*

[8] V. Berger, O. Gauthier-Lafaye, E. Costard, "Photonic band gaps and holography", *J. Appl. Phys., vol. 82, pp. 60-64, July 1997.*

[9] C.J.M. van Rijn, G.J Veldhuis, S. Kuiper: Nanosieves with microsystem technology for microfiltration applications, *Nanotechnology, vol. 9 pp. 343–345, 1998.*

[10] J. Orloff: High-resolution focussed ion beams, *Rev. Sci. Instrum., vol. 64, pp. 1105-1130, 1993.*

[11] A.J. DeMarco, J. Melngailis: Lateral growth of focused ion beam deposited platinum for stencil mask repair, *J. Vac. Sci. Technol. B, vol. 17, pp. 3154-3157, 1999.*

[12] L. Vogelaar, W. Nijdam, H.A.G.M. van Wolferen, R.M. de Ridder, F.B. Segerink, E. Flück, L. Kuipers, N.F. van Hulst: Large area photonic crystal slabs for visible light with waveguiding defect structures: fabrication with focused ion beam assisted laser interference lithography, *Advanced Materials, vol. 13, pp. 1551-1554, October 2001.*

[13] L. Kuipers: Near and far field investigations of photonic structures, *in Proc. ESPC 2002, Warsaw, Poland, April 2002 (this issue).*